Polym. Bull. (2009) 62:629–642
DOI 10.1007/s00289-009-0047-x

ORIGINAL PAPER

Non-isothermal crystallization kinetics of poly (lactic acid)/modified carbon black composite

Zhizhong Su · Weihong Guo · Yongjun Liu · Qiuying Li · Chifei Wu

Received: 21 September 2008 / Revised: 1 February 2009 / Accepted: 2 February 2009 /
Published online: 12 March 2009

Abstract A novel method was employed to modify the surface of carbon black (CB) by an organic small molecule in a Haake Rheomix mixer. Jeziorny equation, the Ozawa model and Mo equation were employed to describe the non-isothermal crystallization process of poly (lactic acid) (PLA), PLA/CB and PLA/modified carbon black (MCB) composites. It is found that the Ozawa model fail to describe the non-isothermal crystallization process for PLA and its composites, while Jeziorny equation and Mo's theory provide a good fitting. The comparison of crystallization kinetics between PLA/MCB and PLA through Lauritzen–Hoffman model indicates that there appears a transition from regimes II to III in PLA and PLA/MCB. The fold surface free energy σ_e of PLA/MCB composite is higher than that of neat PLA, implying that the existence of nucleating agent is unfavorable for the regular folding of the molecule chain.

Introduction

Carbon black (CB) that acted as nucleating agent and increased the crystallization rate has tremendous influence on crystallization of the polymeric matrix [1]. This behavior has been observed in polypropylene/CB composites [2, 3], polyvinylidene fluoride/CB composites, polyamide/CB composites [4], and poly (ethylene terephthalate)/CB composites [5, 6].

Z. Su · W. Guo · Y. Liu · Q. Li · C. Wu (✉)
Polymer Alloy Laboratory, School of Materials Science and Engineering,
East China University of Science and Technology, 200237 Shanghai,
People's Republic of China
e-mail: wucf@ecust.edu.cn

Z. Su
e-mail: suzhizhong530@sohu.com

Poly (lactic acid) (PLA) is a biodegradable polymer, which was widely studied either in biomedical applications or to replace commodity polymers in packaging and other fields where the degradation of the material is an important prerequisite for environmental reasons. It is now attracting much attention because it can be derived from renewable natural resources and is proven to be superior to the conventional petrochemical polymers in regard to the total energy consumption and CO_2 emission in the life cycle assessment. Recently, more attention has been turned to the study of PLA crystallization kinetics [7–11]. In many applications, increasing the crystallization speed of PLA is desired since injection molding of the crystalline PLA, generally gives amorphous products whose modulus greatly drops above the glass transition temperature T_g. This behavior has limited the utility of PLA in the general plastic use, and much effort has been paid to make the injection-molded PLA to crystallize and attain increased heat resistance.

It is well understood that some inorganic fillers (clay, carbon nanotubes, calcium carbonate, etc.), acted as reinforcing agents in polymer composites, can usually induce nucleation for crystallization of matrix [11–14] and accelerate the overall crystallization process. However, there was no literature on CB induced crystallization of PLA. Recently, a new technique was proposed to modify the surface of CB with low molecular weight compound by in situ reaction in our laboratory [15]. The results of thermo gravimetric analysis (TGA), flourier transform infrared spectroscopy (FT-IR) and X-ray photoelectronic spectroscopy (XPS) analysis indicated that organic small molecules were grafted onto the surface of CB [16]. The modified carbon black particles with smaller size were obtained. Moreover, the MCB could be dispersed in polymer or organic solvent stably and uniformly, hence the impact it exert on the crystallization behavior of PLA is desired.

Non-isothermal crystallization kinetics of PLA filled with MCB and CB using different theoretical approaches was described in this paper. Particular attention was paid to the nucleation of MCB on the crystallization of the matrix.

Experimental

Materials

The poly (lactic acid) supplied by NatureWorks was a semi-crystalline grade (PLA 4032D). It comprises around 2% D-LA.

The following Mark-Houwink equation form valid in chloroform [17] at 25 °C was used to determine the molecular weight of PLA:

$$[\eta] = 7.4 \times 10^{-5} M_n^{0.87}$$

The resulting molecular weight of PLA is $M_n = 4.5 \times 10^4$. The CB, N234 was kindly supplied by Cabot Company (USA). The untreated CB has a primary particle size of 30 nm, dibutyl phthalate (DBP) absorption value (ASTM D2414) of 125 mL/100 g, cetyl trimethyl ammonium bromide (CTAB) (ASTM D3765) of 119 m^2/g, iodine number (ASTM D1510) of 120 mg/g. The organic small molecule compound that grafted on CB is 3,9-bis-[1,1-dimethyl-2{-(3-tert-butyl-4-hydroxyl-

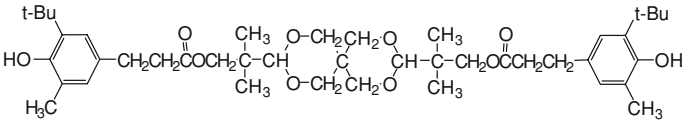

Fig. 1 The molecular structure of AO-80

5-methylphenyl) propionyloxy}ethyl]-2,4,8,10-tertaoxaspiro-[5]-undecane (AO-80), a commercial antioxidant used for polymer(ADK STAB AO-80) and supplied by Asahi Denka Industries Co. (Japan). Its molecular structure was shown in Fig. 1.

Sample preparation

The MCB was prepared in an internal batch mixer (Haake Rheomix600p, German), operating at 140 °C and a rotor speed of 60 rpm according to the patent [15]. CB and AO-80 were pre-mixed at 1/0.8 (wt/wt) ratios, and was then added into the mixer and blended for about 30 min under strong shearing. The mixture was extracted with acetone for 72 h to remove free AO-80.

PLA/CB and PLA/MCB composites were prepared by solution casting. A predetermined amount of filler was added and well dispersed in chloroform solvent by ultrasonic for 10 min. Then PLA was dissolved in the mixed solution having a polymer concentration of 1 g/dl. The mixed solution was cast on a flat glass plate and the solvent was allowed to evaporate at room temperature for approximately 24 h and then dried at 50 °C for 48 h under vacuum. Pure PLA film was prepared for comparation.

Differential scanning calorimetry

Thermal analysis of PLA films and its composites was carried out on a NETZSCH DSC 200PC calorimeter. The calorimeter was calibrated with indium standard. For each measurement, a sample of about 8 mg was placed in an aluminium pan and heated to 200 °C at a heating rate of 10 °C/min, where it was held for 10 min to remove prior thermal history. Then, the melt was cooled to crystallize at selected constant cooling rates β, ranging from 1 to 3 °C/min. It is noteworthy that each sample was used only once and all the runs were carried out under a nitrogen purge.

Polarizing optical microscopy

Spherulite structures were recorded on a polarizing optical microscope (POM) equipped with a METTLER TOLEDO FP90 automatic hot-stage thermal control unit and photographed using a digital camera. Thin film was placed on slide glasses and the thickness of the sample was less than 10 μm. The PLA sample was heated on the hot-stage from room temperature to 200 °C at a heating rate of 20 °C/min, held at 200 °C for 10 min for completion of the polymer melting, rapidly cooled to a desired crystallization temperature (T_c) at a rate of −50 °C/min, and then

crystallized at T_c. For each of the specimens, the average size of spherulite was then measured from the digital image.

Results and discussion

Non-isothermal crystallization process

Non-isothermal crystallization behavior is of more practical interesting than isothermal behavior. This is because polymers are usually processed under non-isothermal cycles rather than in an isothermal condition. Thus, non-isothermal crystallization kinetics of PLA and its composites will be discussed in the following sections.

The non-isothermal crystallization exotherms of neat PLA, PLA/CB and PLA/MCB composites from the melt at different cooling rates are shown in Fig. 2. As the cooling rate increases, the exothermic curve of a given sample becomes wider and shifts to lower temperature. Some of the DSC traces of neat PLA and of the PLA/CB composites display a discontinuity around a temperature range below 120 °C,

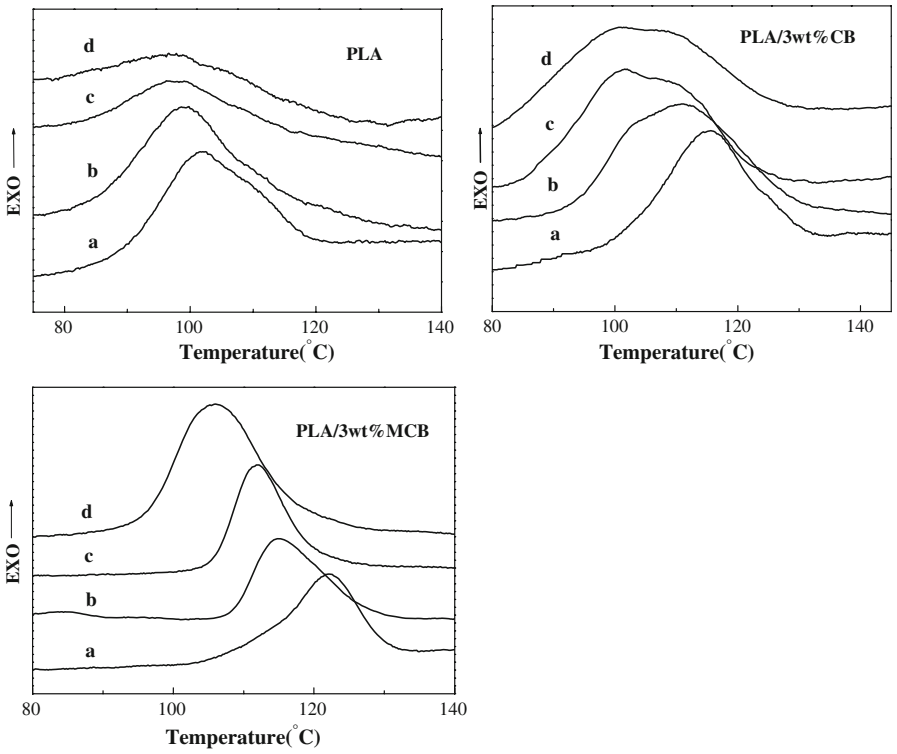

Fig. 2 DSC curves of PLA, PLA/CB, and PLA/MCB in the crystallization process from the melt at various cooling rate: **a** 1 °C/min, **b** 1.5 °C/min, **c** 2 °C/min, **d** 3 °C/min

Table 1 Data of PLA, PLA/CB and PLA/MCB composites from DSC

	β (°C/min)	T_o (°C)	T_c (°C)	$t_{1/2}$ (min)
PLA	1	118.0	101.9	16.0
	1.5	115.2	99.7	12.7
	2	110.6	97.5	8.8
	3	106.4	89.2	7.0
PLA/3 wt%CB	1	125.1	115.3	13.8
	1.5	122.2	110.7	10.9
	2	118.6	103.1	8.6
	3	113.6	98.8	6.5
PLA/3 wt%MCB	1	129.6	122.3	10.1
	1.5	127.9	115.0	8.4
	2	121.2	110.4	6.8
	3	120.3	106.0	5.1

which is caused by a sudden acceleration of the growth of PLA spherulites as described by M. L. Di Lorenzo [8]. The exotherm peak temperatures (T_p), the crystallization onset temperatures (T_o) and other crystallization parameters for the samples are summarized in Table 1. It can be seen that the exotherm peak temperatures of PLA improved significantly as 3 wt% of CB or MCB is added. At a cooling rate of 1 °C/min, for example, addition of CB can improve the exotherm peak temperature from 101.9 to 115 °C, and to 122.3 °C with addition of MCB. Further more, at the same cooling rate, the values of T_o of PLA/CB and PLA/MCB composites are higher than those of neat PLA, indicating that the crystallization processes start earlier in the composites than neat PLA. This means that CB or MCB in PLA is a nucleating agent, and therefore, accelerate the crystallization of PLA. Moreover, the nucleation ability of MCB was higher than that of CB,which can be supposed to be the reduction in particle size and a more uniform distribution of MCB in PLA matrix.

In the non-isothermal crystallization process, the relative crystallinity *X(T)*, a function of crystallization temperature *T*, can be formulated as:

$$X(T) = \int_{T_0}^{T} \left(\frac{dH_c}{dT}\right) dT \Big/ \int_{T_0}^{T_\infty} \left(\frac{dH_c}{dT}\right) dT \quad (1)$$

where T_o and T_∞ represent the temperatures at the onset and the end of the crystallization process, respectively, and dH_c is the enthalpy of the crystallization released during an infinitesimal temperature range dT [18]. The crystallization time (t) can be calculated by the following:

$$t = (T_0 - T)/\beta \quad (2)$$

where T is the temperature at time t, and β is the cooling rate. Figure 3 shows the plots of the relative crystallinity $X(t)$ versus crystallization time t. From these curves, the half-time of crystallization ($t_{1/2}$), can be determined and summarized in Table 1. As shown, $t_{1/2}$ decreases as cooling rate increasing, indicates that the crystallization of the PLA can be conducted fast at higher cooling rate. At mean

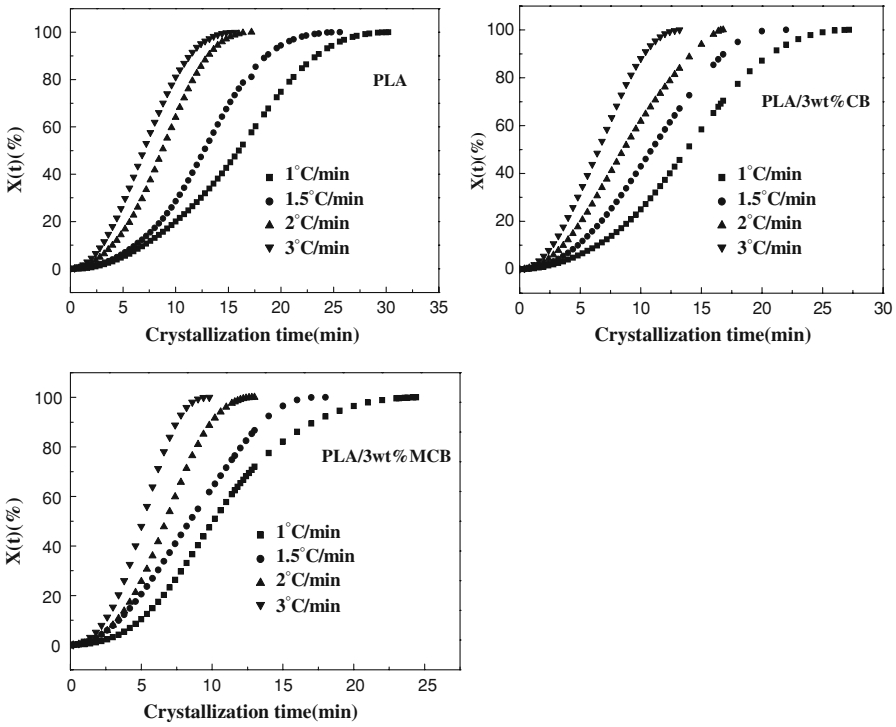

Fig. 3 Plots of $X(t)$ versus crystallization time at different cooling rates

time, the order of $t_{1/2}$ of three samples follow $t_{1/2(\mathrm{PLA})} > t_{1/2(\mathrm{PLA/CB})} > t_{1/2(\mathrm{PLA/MCB})}$, clearly show us that the crystallization rate of PLA has been significantly accelerated after addition of CB or MCB.

Non-isothermal crystallization kinetics

Avrami equation was also employed to describe the primary stage of non-isothermal crystallization [19–21].

$$1 - X(t) = \exp(-Zt^n) \tag{3}$$

$$\log[-\ln(1 - X(t))] = \log Z + n\log t \tag{4}$$

where $X(t)$ is the relative degree of crystallinity at the time t, Z the crystallization rate constant and n is the Avrami exponent in the non-isothermal crystallization process. Considering the non-isothermal character of the process investigated, Jeziorny suggested that the value of Z, should be adequately revised using the cooling rate, β, as follows [22]:

$$\log Z_c = (\log Z)/\beta \tag{5}$$

where Z_c is the revised crystallization rate constant. Plotting $\log[-\ln(1 - X(t))]$ versus $\log t$, a straight line should be obtained, Z and n correspond to the intercept

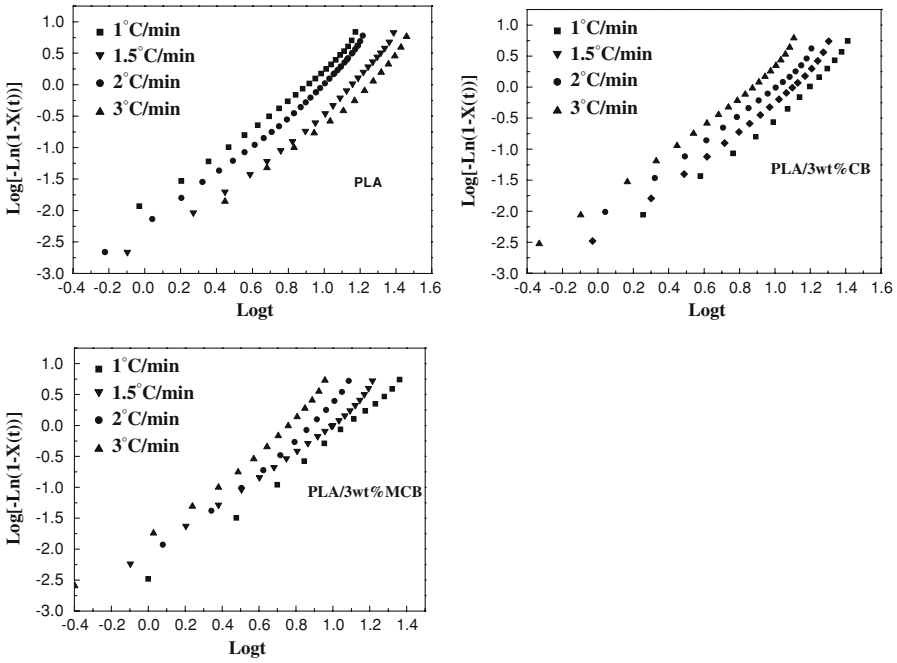

Fig. 4 Plots of $\log[-\ln(1 - X(t))]$ versus $\log t$ for PLA and its composites

and slope of the line respectively. Figure 4 displays the plots of $\log[-\ln(1 - X(t))]$ versus $\log t$ for PLA, PLA/CB, and PLA/MCB composites at different cooling rates.

As shown in Fig. 4, for all samples, there are two stages of crystallization at a given cooling rate. The initial part ($\log[-\ln(1 - X(t))] < 0$) shows a linear relationship and Z and n can be calculated. It shows that Avrami analysis works well for a large part of non-isothermal crystallization. In fact, consecutively non-isothermal crystallization can only rarely realized since the sample's internal temperature is constant for a certain time, that is because the heat of fusion which is released in the sample's internal balances the externally enforced cooling. At the second stage the curves deviate from the linear relationship suggesting secondary crystallization and spherulite impingement.

n, and Z_c of PLA, PLA/CB, and PLA/MCB composites calculated from the linear parts (i.e. initial parts: $\log[-\ln(1 - X(t))] < 0$) are collected in Table 2. The values of n for virgin PLA and its composites are around 2.0, suggesting that the primary crystallization process might correspond to a two dimensional circular diffusion controlled growth. The values of Z_c for PLA/CB and PLA/MCB composites are larger than those of PLA at same cooling rate, meaning a much higher crystallization rate for PLA in the composites. Similarly, the crystallization rate of PLA/MCB is faster than that of PLA/CB, in agreement with the results of $t_{1/2}$.

Table 2 Results of the Avrami analysis for non-isothermal crystallization of PLA and its composites PLA/CB and PLA/MCB

Samples	Avrami parameters	Cooling rate (°C/min)			
		1	1.5	2	3
PLA	n	2.2	1.9	1.7	1.7
	Z_c	1.32×10^{-3}	0.023	0.0794	0.244
PLA/3 wt%CB	n	2.1	2.1	2.2	1.9
	Z_c	2.45×10^{-3}	0.0257	0.084	0.244
PLA/3 wt%MCB	n	1.7	2.0	2.1	2.0
	Z_c	3.39×10^{-3}	0.0437	0.0912	0.251

Ozawa analysis in non-isothermal crystallization kinetics

It is well known that Avrami equation can describe the isothermal crystallization process. The Avrami equation for a non-isothermal crystallization process may be considered as just the same mode for an isothermal crystallization process, but it does not take into account of the factors that are special for non-isothermal processes, i.e. cooling rate and the temperature variation at different time. Considering the effect of cooling rate on non-isothermal crystallization, Ozawa [23] modified the Avrami equation by incorporating the cooling rate factor as follows:

$$\log[-\ln(1 - X(T))] = \log P(T) - m\log\beta \tag{6}$$

where $P(T)$ is the cooling function related to the overall crystallization rate and m is the Ozawa exponent. Figure 5 shows the plots of $\log\{-\ln[1 - X(T)]\}$ versus $\log \beta$ at various temperatures for PLA and its composites. There are no straight lines obtained, indicating that the Ozawa model fail to describe non-isothermal crystallization in both neat PLA and its composites. The Ozawa equation was derived from the Avrami theory, in which secondary crystallization and impingement of spherulites were ignored. However, at a given temperature, the crystallization processes at different cooling rates are at different stages, that is, the lower cooling rate process is toward the end of the crystallization process, whereas at the higher cooling rate, the crystallization process is at an early stage. This phenomenon is more evident when the difference of β is large [24].

Combining Avrami equation and the Ozawa equation

In order to find a method to describe exactly the non-isothermal crystallization process, Mo et al. [25] suggested a novel kinetic approach by combining the Avrami equation (Eq. 3) with the Ozawa equation (Eq. 6).

$$\log Z + n\log t = \log P(T) - m\log\beta \tag{7}$$

$$\log\beta = \log F(T) - \alpha\log t \tag{8}$$

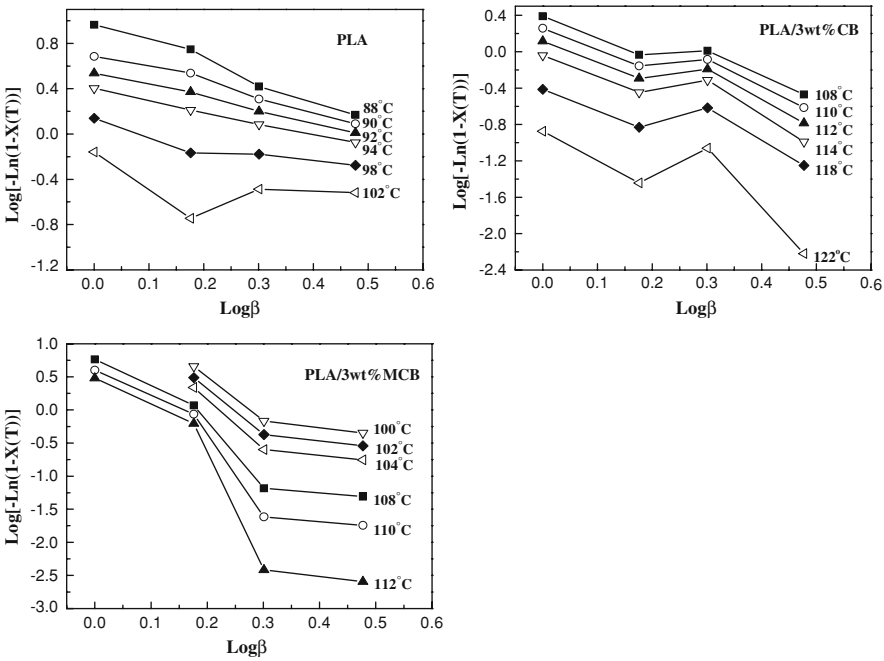

Fig. 5 Plots of $\log\{-\ln[1 - X(T)]\}$ Versus $\log \beta$ for PLA and its composites

here, $F(T)(=[P(T)/Z]1/m)$ is the kinetics parameter, referring to the value of cooling rate that has to be chosen at the unit crystallization time when the measured system amounts to a certain degree of crystallinity, and α is the ratio of the Avrami exponent n to the Ozawa exponent m.

The plots of $\log \beta$ versus $\log t$ for PLA, PLA/CB, and PLA/MCB at different relative crystallinity are shown in Fig. 6. Clearly, Mo's method can well describe the non-isothermal crystallization for all of them. $F(T)$ and α, achieved from the intercept and the slope in Fig. 6, respectively, are summarized in Table 3. The range of α value is 1.262–1.435 for neat PLA and 1.260–1.544 for PLA/CB, 1.275–1.66 for PLA/MCB composites, while $F(T)$ increases with the relative crystallinity increasing. This reveals that incorporation of CB or MCB into the PLA matrix affects slightly the mechanism of nucleation and crystal growth of PLA. For the same relative crystallinity, the $F(T)$ of PLA is the highest, and that of PLA/MCB is the lowest, which means that the crystallization rate of PLA/MCB is the fastest, in well agreement with the statement made from the modified Avrami analysis and $t_{1/2}$.

Spherulite growth rate and fold surface free energy

The Hoffman–Lauritzen theory for spherulite growth considers two processes occurring at the growth front. The first process is the deposition of a secondary nucleus on the growth face and the second process is the subsequent growth along

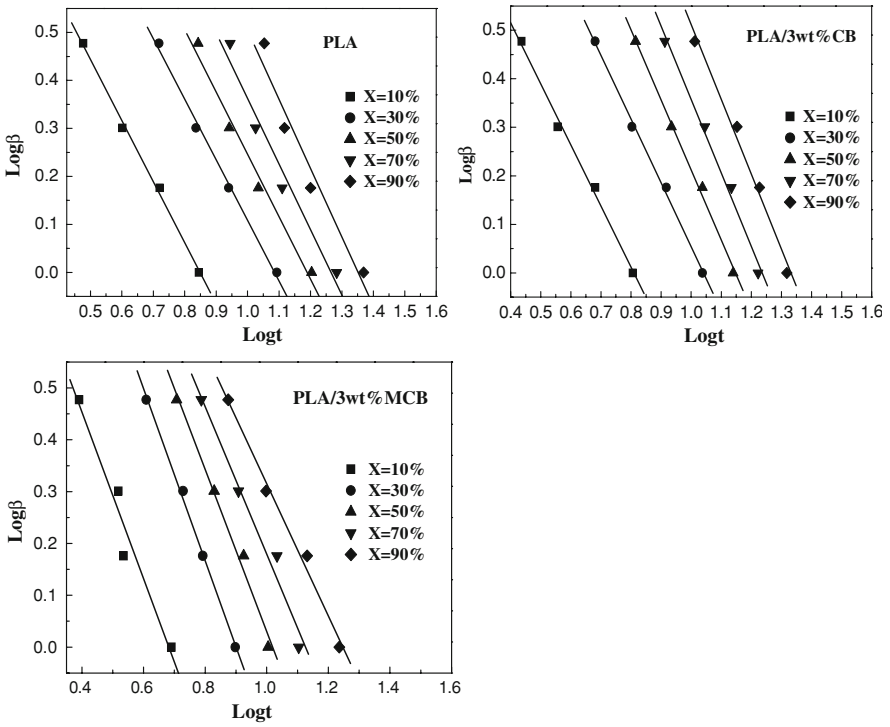

Fig. 6 Plots of log β versus log t for PLA, PLA/CB, and PLA/MCB at different relative crystallinity

the face at the niches formed by the secondary nucleus [26]. The general logarithmic form of the secondary nucleation theory is

$$\ln G + \frac{U^*}{R(T_c - T_\infty)} = \ln G_0 - \frac{K_g}{T_c \Delta T f} \tag{9}$$

where G is the linear growth rate, U^* is the activation energy for transport of macromolecules in the melt, R is the gas constant, T_c is the crystallization temperature, T_∞ is the temperature at which all motions associated with viscous flow cease and is taken as $T_g - C$. In addition, G_0 is the pre-exponential factor and ΔT is the degree of undercooling, $\Delta T = T_m^\circ - T_c$ where T_m° is the equilibrium melting temperature, evaluated by a Hoffmann–Week analysis; f is a corrective factor that takes into account the variation of the equilibrium melting enthalpy with temperature, defined as $f = 2T_c/(T_c + T_m^\circ)$; The nucleation constant K_g is a term connected with the energy needed for the formation of nuclei of critical size, and is defined as:

$$K_g = \frac{nb\sigma\sigma_e T_m^o}{\Delta H_f k} \tag{10}$$

where $n = 4$ for regimes I and III and $n = 2$ for regime II, b is the thickness of the crystal stem added on the substrate, σ is the lateral surface free energy, σ_e is the

Table 3 Non-isothermal crystallization kinetic parameters at different relative degrees of crystallinity by Mo method

	X(%)				
	10%	30%	50%	70%	90%
PLA					
F(*T*)	12.02	31.41	39.26	53.33	87.10
α	1.274	1.262	1.30	1.364	1.435
PLA/3 wt%CB					
F(*T*)	12.59	23.44	45.19	74.13	114.02
α	1.26	1.32	1.44	1.514	1.544
PLA/3 wt%MCB					
F(*T*)	10.47	23.44	35.08	40.09	38.90
α	1.606	1.66	1.564	1.42	1.275

surface fold free energy, k is the Boltzmann constant, and ΔH_f is the heat of fusion of the PLA crystal.

In order to study the crystallization regimes in the temperature range investigated, the spherulite growth rate was plotted according to $\log G + U^*/2.303R(T_c - T_\infty)$ versus $1/T_c\Delta Tf$. For the calculations, values of $T_m^o = 174$ °C evaluated by Hoffmann–Week analysis and $T_g = 60.8$ °C were used. To fit experimental data, $U^* = 1{,}500$ cal/mol and $T_\infty = T_g - 30$ K were utilized. Isothermal spherulitic growth of PLA and PLA/MCB composite exhibited a linear increase in spherulite radius with time until impingement, the slope of the plots provided the linear growth rate G. The results of Hoffman–Lauritzen treatment using the G values presented in Fig. 7 are illustrated in Fig. 8. The data of PLA present three lines between 87 and 150 °C, if one considers G data taken between 85 and 118 °C, and between 132 and 150 °C, as two independent sets of data, the slope ratio of the two lines is equal to 2 in good agreement with the value predicted by the theory [26]. In this regard, a transition can be observed around 125 °C, a temperature range from 120 to 130 °C, corresponding to the third line in Fig. 8. As mentioned above, the discontinuity around a temperature range can be attributed to a sudden acceleration of the growth of PLA spherulites. For the PLA/MCB composite containing 3 wt% content of MCB, the similar phenomena can be found, but the data present two lines and the transition temperature observed around 130 °C. Acting as nucleating agent, MCB makes PLA approach the highest crystallization rate ahead.

The slopes of these two linear trendlines, K_g, calculated in different regimes are list in Table 4. Using $\Delta H_f = 11.11 \times 10^8$ erg/cm^3 and layer thickness $b = 5.17 \times 10^{-10}$ m [27], we calculated $\sigma\sigma_e$, then estimated the lateral surface energy, σ, using Thomas–Stavely equation

$$\sigma = 0.25\Delta H_f b \tag{11}$$

The σ value was then calculated as 1.44×10^{-2} J m^{-2} for PLA and PLA/MCB composite. Substitution of this value into $\sigma\sigma_e$ permitted estimation of the fold

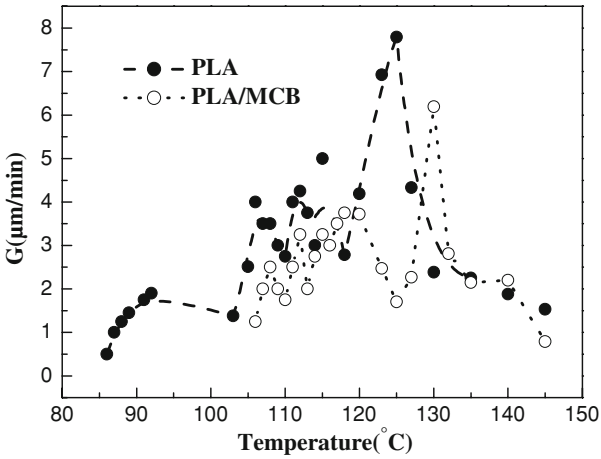

Fig. 7 Spherulite growth rates measured at isothermal conditions for PLA and PLA/MCB crystallized at different temperatures

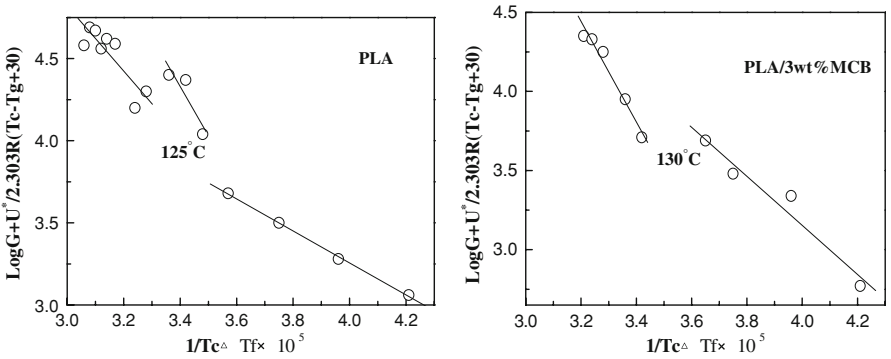

Fig. 8 Kinetic analysis of nonisothermal and isothermal growth data of PLA and PLA/MCB under $U^* = 1{,}500$ J/mol and $T_\infty = T_g - 30$ K

Table 4 Various parameters determined by crystallization kinetic analysis for PLA and PLA/MCB

Sample	$K_g \times 10^{-5}$ K^2	$\sigma\sigma_e \times 10^6$ (J^2 m^{-4})	Remarks
PLA	1.98	306	Regime III
	0.97	300	Regime II
PLA/MCB	3.17	490	Regime III
	1.55	479	Regime II

surface free energy, σ_e, 2.11×10^{-2} J m^{-2} for PLA and 3.38×10^{-2} J m^{-2} for PLA/MCB composite.

The value of σ_e for PLA/MCB composite is higher than that of PLA, indicating MCB probably hinders the chain flexibility and consequence makes crystal growth slower. Considering the regime II/III transition temperature shifting toward high

temperature, it is reasonable to believe that MCB has a stronger effect on surface nucleation than on crystal growth, and thus, MCB promote the overall crystallization rate of PLA.

Conclusions

CB and MCB act as nucleating agents for PLA, the nucleation ability of MCB is higher than that of CB. Ozawa model fail to describe the non-isothermal crystallization process for PLA and its composites, while Mo's theory provide a good fitting. The comparison of crystallization kinetics between PLA/MCB and PLA through Lauritzen–Hoffman model indicates that there appears a transition from regimes II to III in PLA and PLA/MCB composites. The fold surface free energy σ_e of PLA/MCB composite is higher than that of neat PLA, implying that the existence of MCB is unfavorable for the regular folding of the molecule chain, the crystal growth slower as the chain flexibility is hindered by MCB. MCB has a stronger effect on surface nucleation than on crystal growth, and thus, promote the overall crystallization rate of PLA.

Acknowledgments The authors are grateful for the financial supports of the Key Project of National Natural Science Foundation of China (No. 50733001).

References

1. Mucha M, Marszalek J, Fidrych A (2000) Crystallization of isotactic polypropylene containing carbon black as a filler. Polymer 41:4137
2. Mucha M, Krolikowski Z (2003) Application of DSC to study crystallization kinetics of polypropylene containing fillers. J Therm Anal Cal 74:549
3. Wiemann K, Kaminsky W, Gojny FH, Schulte K (2005) Synthesis and properties of syndiotactic poly(propylene)/carbon nanofiber and nanotube composites prepared by in situ polymerization with metallocene/MAO catalysts. Macromol Chem Phys 206:1472
4. Del Ria C, Ojeda MC, Acosta JL (2000) Carbon black effect on the microstructure of incompatible polymer blends. Eur Polym J 36:1687
5. Kim D, Seo K, Hong K, Kim S (1999) Effects of dispersing agents on dspersity and mechanical properties of carbon black/PET. Polym Eng Sci 39:500
6. Fechine GJM, Rabello MS, Souto-Maior RM (2002) Structural changes during photodegradation of poly(ethylene terephthalate). Polym Degrad Stab 75:153
7. Urayamaa H, Kanamori T, Fukushima K, Kimura Y (2003) Controlled crystal nucleation in the melt-crystallization of poly(L-lactide) and poly(L-lactide)/poly(D-lactide) stereocomplex. Polymer 44:5635
8. Di Lorenzo ML (2005) Crystallization behavior of poly(L-lactic acid). Eur Polym J 41:569
9. Miyata T, Masuko T (1998) Crystallization behaviour of poly(L-lactide). Polymer 39:5515
10. He Y, Fan ZY, Hu YF, Wu T, Wei J, Li SM (2007) DSC analysis of isothermal melt-crystallization, glass transition and melting behavior of poly(l-lactide) with different molecular weights. Eur Polym J 43:4431
11. Fornes TD, Paul DR (2003) Crystallization behavior of nylon 6 nanocomposites. Polymer 44:3945
12. Wang B, Sun G, Liu J, He X, Li J (2006) Crystallization behavior of carbon nanotubes-filled polyamide 1010. J Appl Polym Sci 100:3794
13. Lin Z, Huang Z, Zhang Y, Mai K, Zeng H (2004) Crystallization and melting behavior of nano-$CaCO_3$/polypropylene composites modified by acrylic acid. J Appl Polym Sci 91:2443

14. Grozdanov A, Buzarovska A, Bogoeva-Gaceva G, Nedkov E (2005) Nonisothermal melting and crystallization of polypropylene in model composites: kinetic analysis. J Polym Sci Part B: Polym Phys 43:66
15. Wu C, Zhou X, Zhang X, Xu H, Li H, Li X, Zhang L (2004) Chin Pat CN1781999
16. Chen J, Li X, Wu C (2007) Crystallization behavior of polypropylene filled with modified carbon black. Polym J 39:722
17. Rafler G, Dahlmann J, Wiener K (1990) Biologisch abbaubare polymere. 1. Mitt. Viskositäts-molmassen-beziehung für poly-d,l-lactid und poly(glycolid(50)-co-lactid(50)). Acta Polym 41:328
18. Cebe P, Hong S (1986) Crystallization behaviour of poly(ether-ether-ketone). Polymer 27:1183
19. Avrami M (1939) Kinetics of phase change. J Chem Phys 7:1103
20. Avrami M (1940) Kinetics of phase change. J Chem Phys 8:212
21. Wunderlich B (1976) Macromolecular physics. Academic Press, New York
22. Jeziorny A (1978) Parameters characterizing the kinetics of the non-isothermal crystallization of poly(ethylene terephthalate) determined by d.s.c. Polymer 19:1142
23. Ozawa T (1971) Kinetics of non-isothermal crystallization. Polymer 12:150
24. Cebe P (1988) Non-isothermal crystallization of poly(etheretherketone) aromatic polymer composite. Polym Comp 9:271
25. Liu T, Mo Z, Wang S, Zhang H (1997) Nonisothermal melt and cold crystallization kinetics of poly(aryl ether ether ketone ketone). Polym Eng Sci 37:568
26. Hoffman JD, Davis GT, Lauritzen Jr JI (1976) In: Hannay NB (ed) Treatise on solid state chemistry, chap 7, vol 3. Plenum Press, New York
27. Vasanthakumari R, Pennings A (1983) Crystallization kinetics of poly (L-lactic acid). J Polym 24:175